Supplementary Information for Phosphatidylserine Reversibly Binds Cu^{2+} with Extremely High Affinity

Christopher F. Monson, Xiao Cong, Aaron Robison, Hudson P. Pace, Chunming Liu, Matthew F. Poyton, and Paul S. Cremer

Department of Chemistry, Texas A&M University, 3255 TAMU, College Station, Texas 77843, United States

April 2, 2012

Microfluidic Device

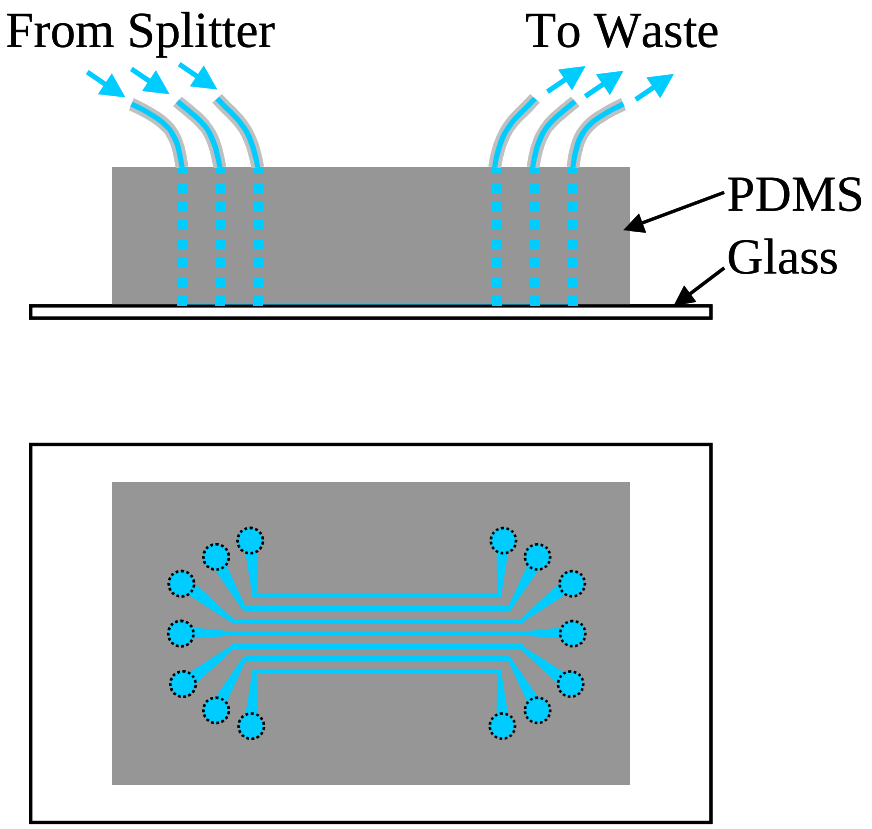

Figure S1. The microfluidic device consisted of a patterned PDMS block adhered to a glass coverslip. Buffer supply tubes from the flow splitter (schematic diagram shown in Figure S2) lead into the microfluidic device. The fabrication procedure for this microfluidic device was described in the experimental section.

Flow Splitter Device

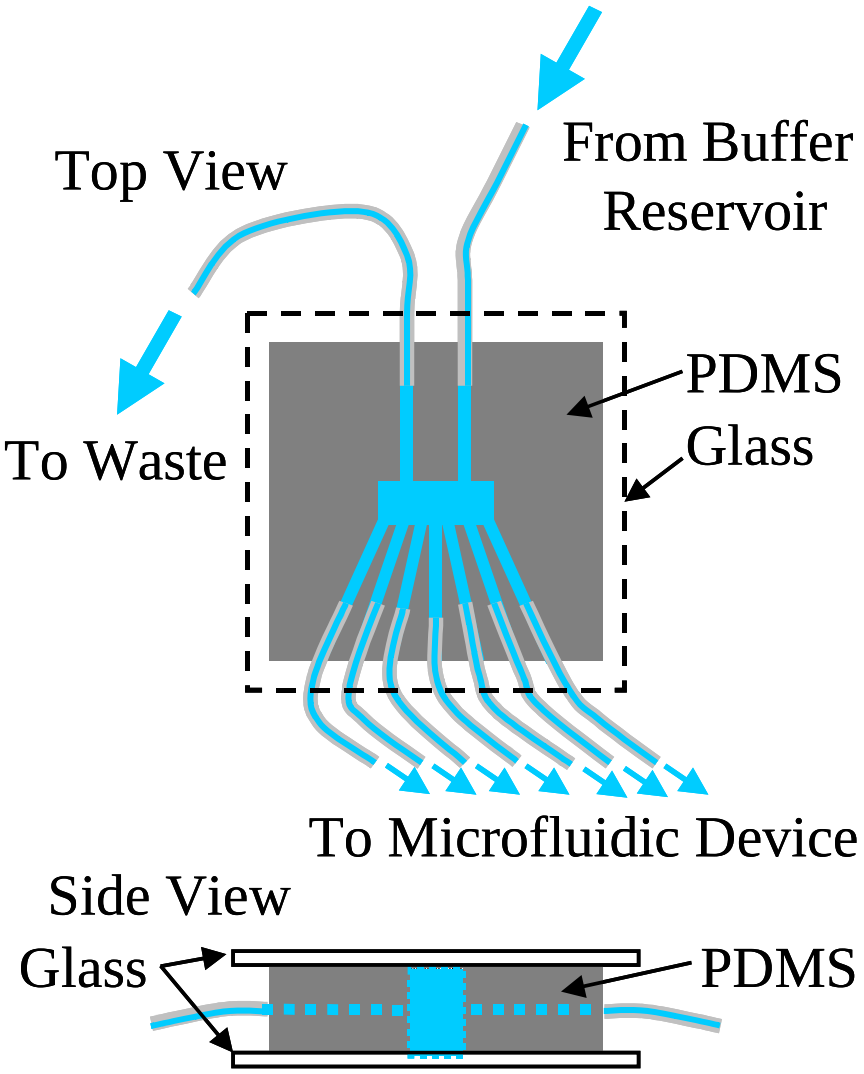

Figure S2. The flow splitter splits the gravity driven flow from a single line from a buffer reservoir into a waste line and up to seven supply lines that feed into a microfluidic channel array. The flow splitter also catches any bubbles introduced during buffer exchange.

UV/Vis Absorbance (top) and Fluorescence Emission (bottom) of Vesicles in the Presence and Absence of $CuSO_4$

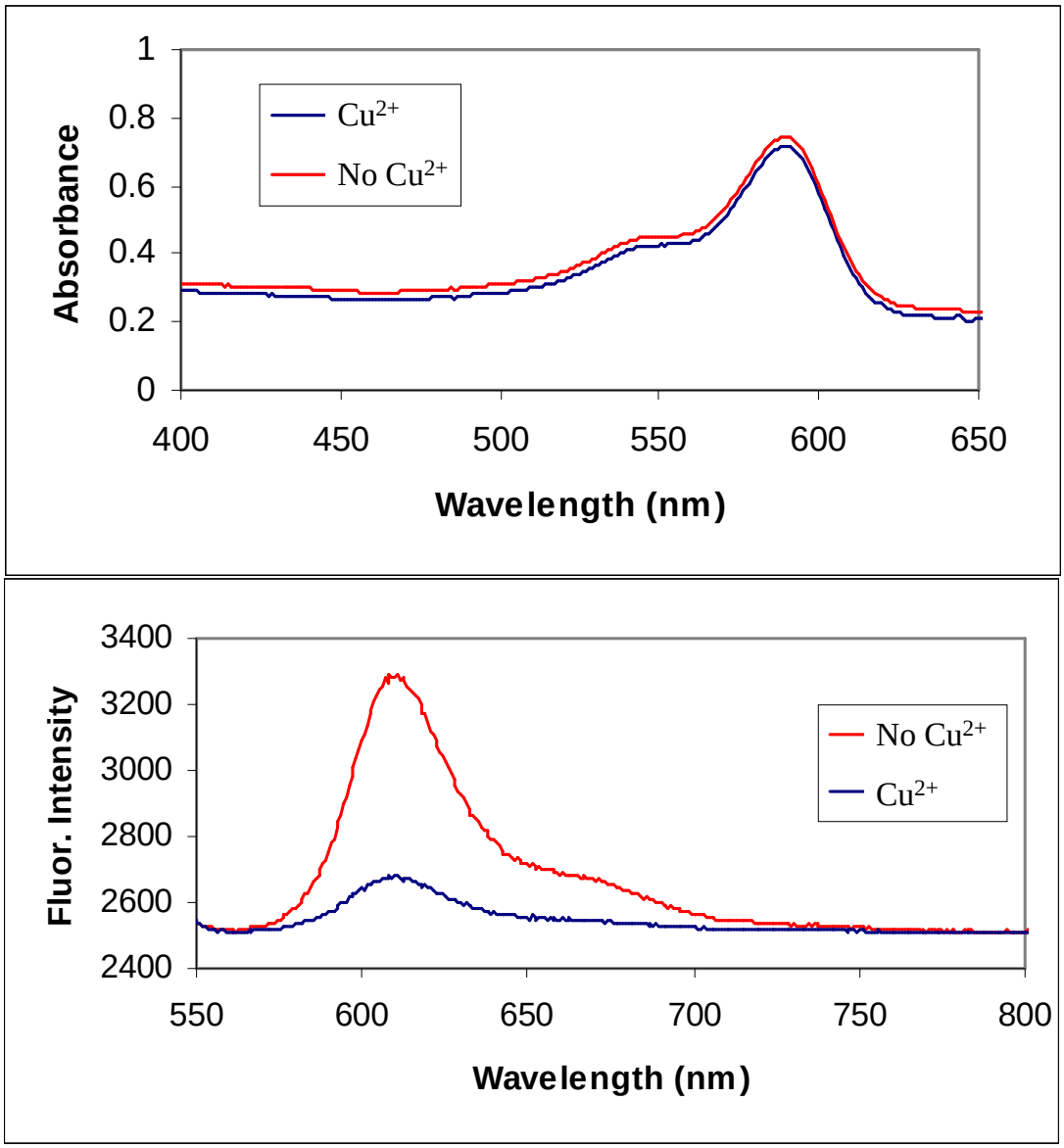

Figure S3. (top) Absorbance and (bottom) fluorescence emission spectra of 100 nm vesicles composed of 1 mol% TR-DHPE, 15 mol% DOPS and 84 mol% POPC at 1 mg/mL. The experiments were performed in 10 mM Tris buffer containing 100 mM NaCl, at pH 7.4. The red spectra show no addition of $CuSO_4$, while the blue spectra were taken with the addition of 100 μM $CuSO_4$ (saturated at 1:2 Cu^{2+}:PS complex). Fluorescence excitation was performed at ~525 nm. Since the adsorption did not shift, while the fluorescence was substantially quenched, a static quenching mechanism can be ruled out.[1,2] Instead, the mechanism should involve dynamic quenching.

Quenching data with Hill equation fit

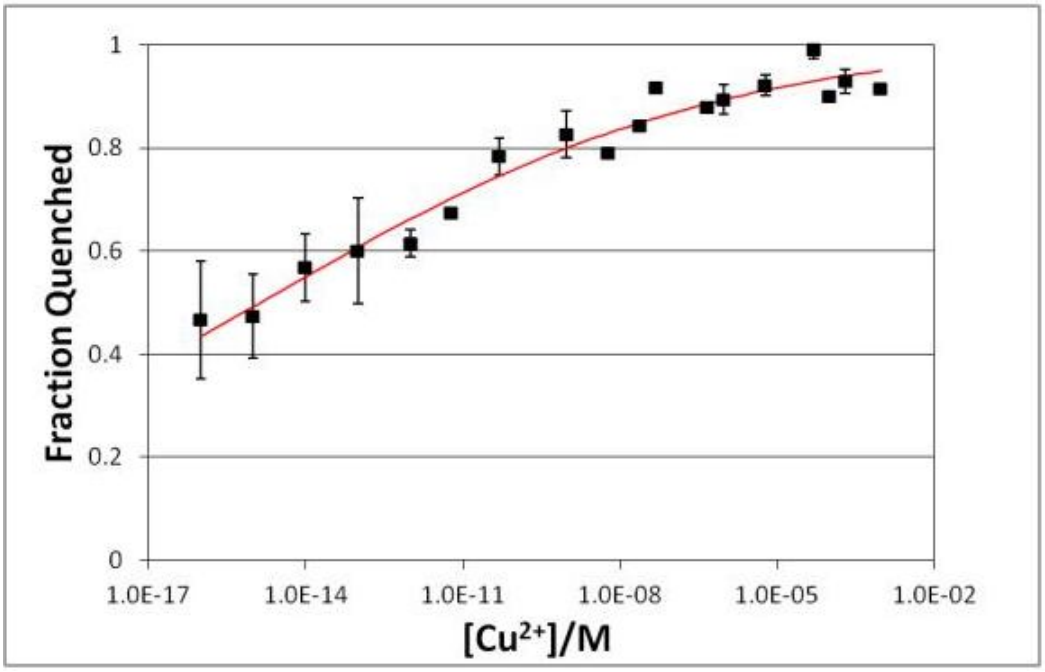

Figure S4. The data shown from Figure 4 along with a fit of the data by the Hill equation[3,4]:

$$\Delta F = \Delta F_{\max} \times \frac{([L])^n}{([L])^n + (K_d)^n}$$

where ΔF is the fraction of dye that is quenched by the Cu^{2+}-PS complex (1 minus the normalized intensity), $\Delta F_{\max}$ is the maximum fraction quenched, $[L]$ is the bulk Cu^{2+} concentration, K_d is the apparent equilibrium dissociation constant, and n is the Hill coefficient of cooperativity.[3,4] The data was fit in Origin 7.5 and the K_d value obtained was 1.8×10^{-15} M with an error of 1.7×10^{-15} M. It should be noted that this fit has the greatest R^2 value = 0.96 and the lowest chi-square test value = 0.0012. $\Delta F_{\max} = 1.01 \pm 0.046$ while the Hill coefficient $n = 0.10 \pm 0.016$. As noted in the main text, the last four points have the greatest error bars and the purity is the water sample is difficult to characterize at femtomolar concentrations even by ICP-MS. Therefore, if trace Cu^{2+} was present in the background of the lowest four concentration it would shift the apparent fit to a tighter value. As such 1.8×10^{-15} M probably represents a lower bound for the equilibrium dissociation constant. On the other hand, the signal to noise is already quite good at 1×10^{-12} M and impurties can be easily tested at this level by ICP-MS. As such, this value is probaby beyond the upper bound and the dissociation constant should be less than this and in the femtomolar range.

Job's Plot Measurements

The Job's method[5] of continuous concentration variation was applied to determine the binding stoichiometry between PS and Cu^{2+}. Experiments were performed in Tris/NaCl buffer (10 mM Tris, 100 mM NaCl, pH 7.4). 100 nm POPC vesicles containing 1 mol% TR-DHPE, 0 to 15 mol% DOPS at 0.17 mg/mL were used and serial concentrations of $CuSO_4$ ranging from 0 to 33 μM were added during vesicle extrusion. The total molar concentration of PS and Cu^{2+} was held constant at 33 μM, while their mole fractions were varied. The fraction of the quenched fluorescence, which is related to the amount of complex formed, was plotted against the mole fraction of Cu^{2+}. The inflection points of the Job's plot yielded the binding stoichiometry of the complexes formed. As can be seen, the maximum in fluorescence quenching occurred when the mole fraction of Cu^{2+} was about 0.33. This is consistent with 1:2 binding for the Cu^{2+}:PS complex.

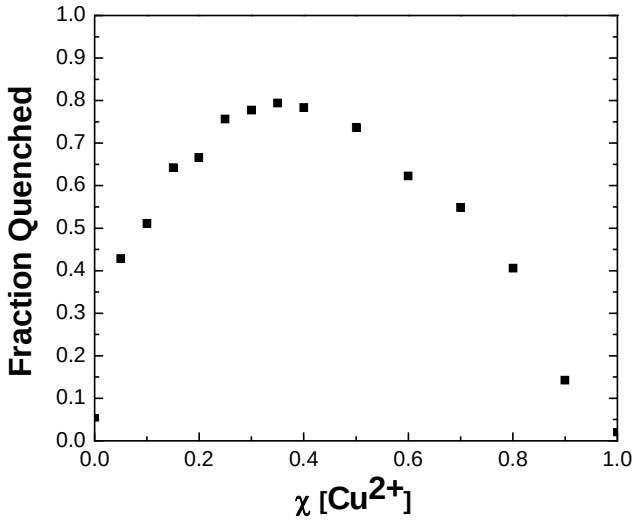

Figure S5. A Job's plot shows the binding stoichiometry of the complexes formed, which corroborates the Stern-Volmer plot in Figure 5.

EPR Spectra of PS Vesicles, $CuSO_4$ and PS Vesicles with $CuSO_4$ in buffer.

EPR spectra were collected on an X-Band Bruker EMX Spectrometer (Bruker Biospin, Billerica, MA) with an Oxford ESR900 liquid Helium cryostat.

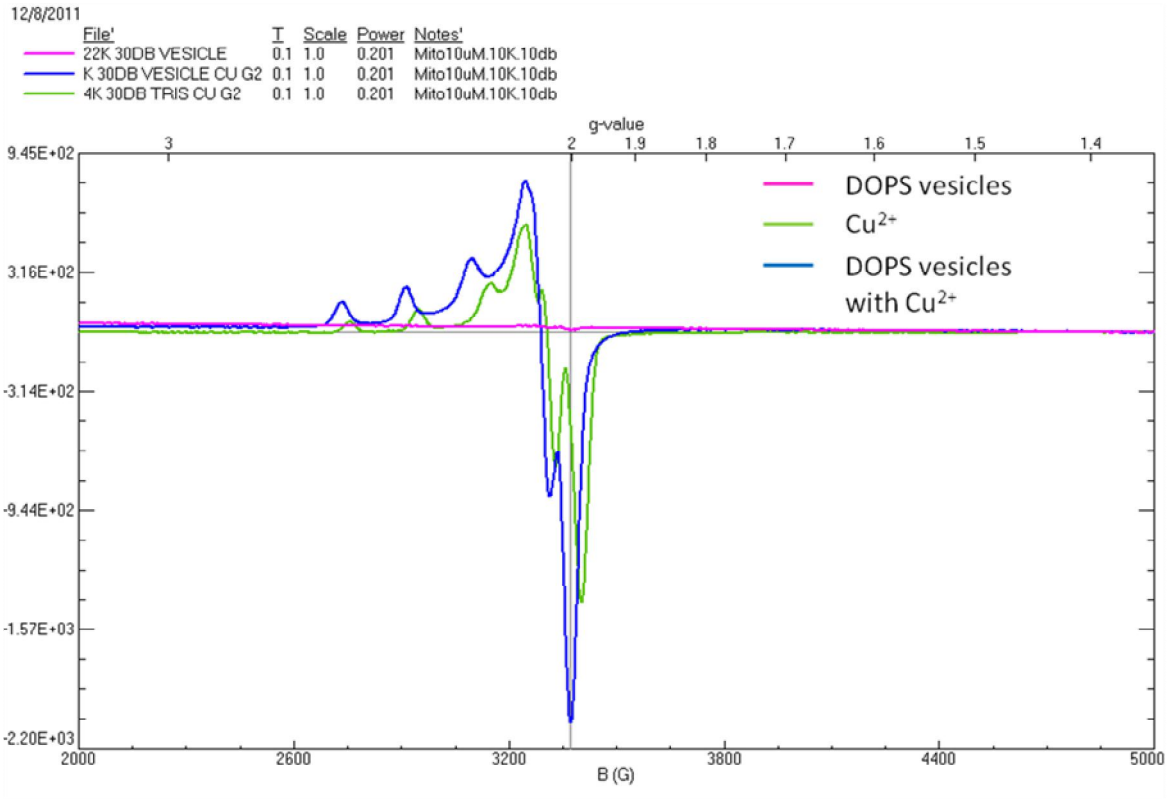

Figure S6. EPR spectra of 100 nm vesicles containing 15 mol% DOPS in POPC (pink), $CuSO_4$ (green), and DOPS vesicles with $CuSO_4$ (blue, saturated at 2:1 PS:Cu^{2+} complex) in Tris/NaCl buffer. 10 mM Tris and 100 mM NaCl buffer at pH 7.4 were used. The $g_{\|}$ value of Cu^{2+} with vesicles is 2.252 and $A_{\|}$ value is 171 gauss = $180 \cdot 10^{-4}$ cm^{-1} (blue), which is similar to the EPR spectra data of CuL_2 complexes such as with O-phospho-L-serine.[6,7] Indeed, the shift in the EPR signal when adding PS vesicles shows that a change in copper complexation took place.

Metal Ion Quenching of TR-DHPE with vesicles containing no PS

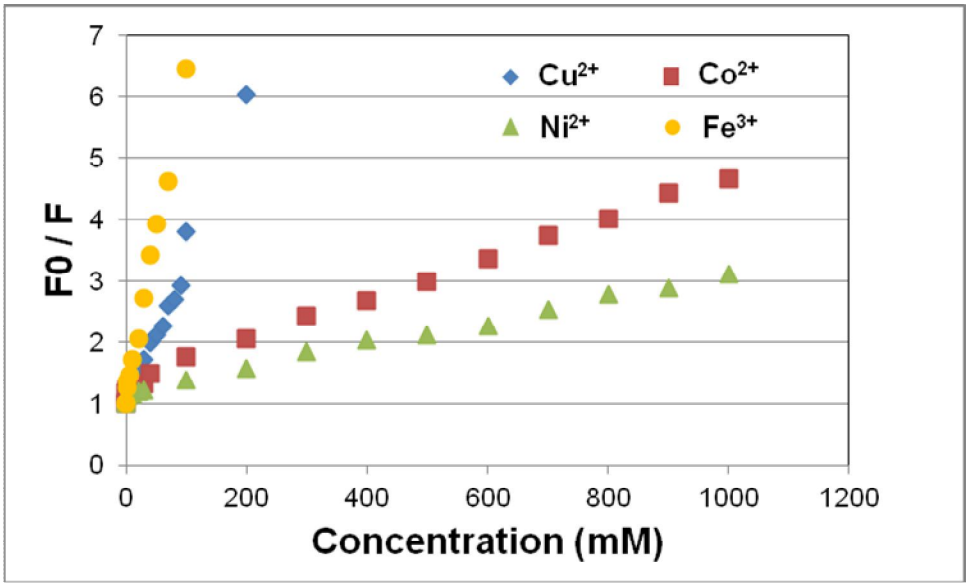

Figure S7. Stern-Volmer plots of the metal ion quenching of 100 nm POPC vesicles containing 1 mol% TR-DHPE. Various metal ions as chloride salts were added into vesicle solution in 1 M Tris with 100 mM NaCl at pH 7.4. As no PS was present, the quenching was due only to direct metal ion interactions with fluorophores and the concentrations of Cu^{2+} required for quenching was 9 orders of magnitude higher or more. Additionally, Ca^{2+}, Mg^{2+}, Ba^{2+}, Zn^{2+}, Cd^{2+} and Hg^{2+} were tested and found to result in no measurable quenching up to 10 mM concentrations.

DOPS vs DPPS Fluorescence Quenching

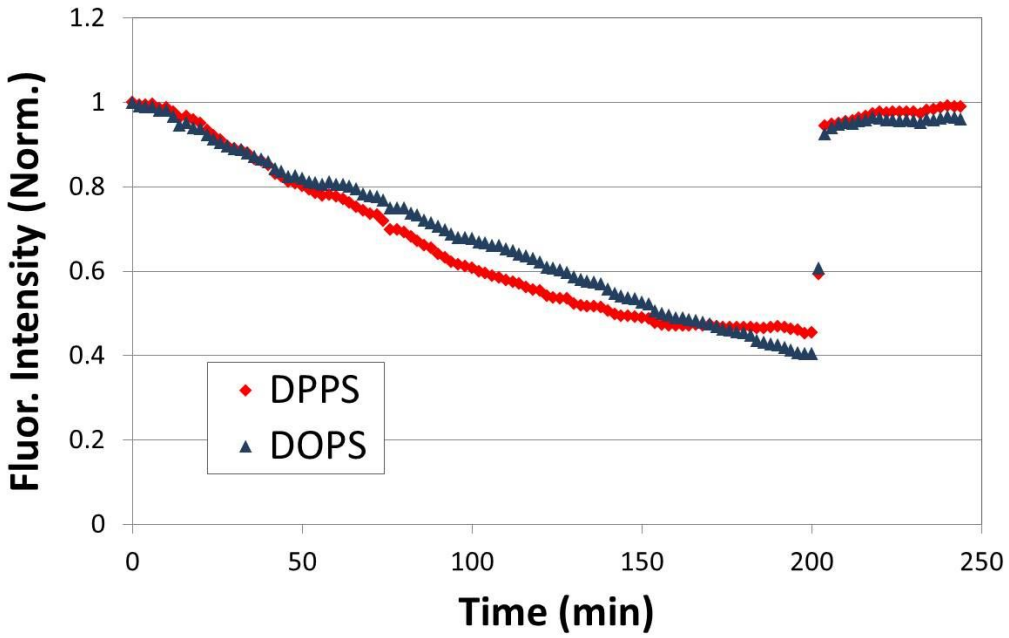

Figure S8. Quenching of TR-DHPE on SLBs by DPPS (red) or DOPS (blue) with 1 pM $CuCl_2$ present in 1 mM citrate/MES/Tris buffer at pH 8.0. The SLBs consisted of 1 mol% TR-DHPE and 20 mol% DPPS or DOPS in POPC. After 200 min, the buffer was changed to acidic pH (pH=3.1) to observe the reversible dequenching process.

Protein-bound Fluorescence Response to DOPS

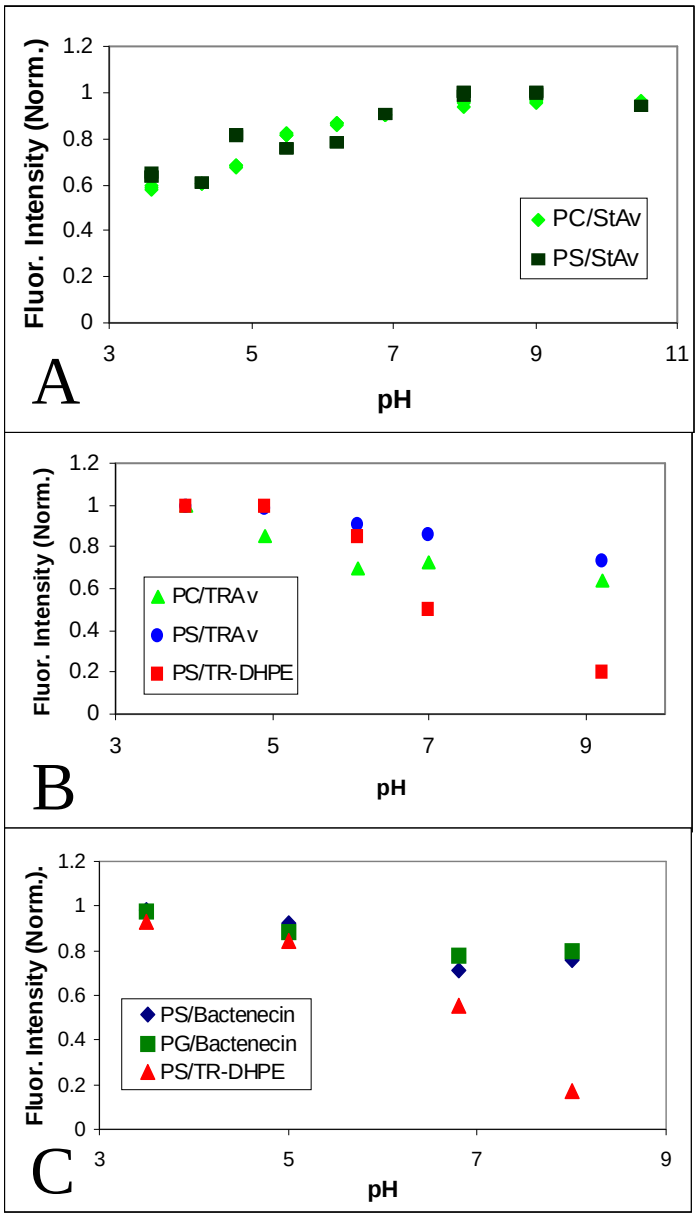

Figure S9. (A) The fluorescence response of supported bilayers in microfluidic channels after flowing in Alexa 488-labeled streptavidin (StAv), (B) Texas Red-labeled avidin (TRAv) and (C) a rhodamine-labeled bactenecin derivative peptide as a function of pH. The data were taken with 100 nM $CuSO_4$ in the presence of 20 mol% DOPS (where PS is indicated) in POPC with a 10 mM citric acid/tris buffer adjusted to the appropriate pH with HCl and NaOH. The avidin and streptavidin bound to biotinylated DOPE, present at 1 mol% in the supported bilayers. The bactenecin was added at 20 µM and spontaneously bound to the SLBs. In the PG/Bactenecin experiment, POPG was present at 20 mol% in the control experiment (green squares in C).

FRAP Data for PS and No PS SLBs

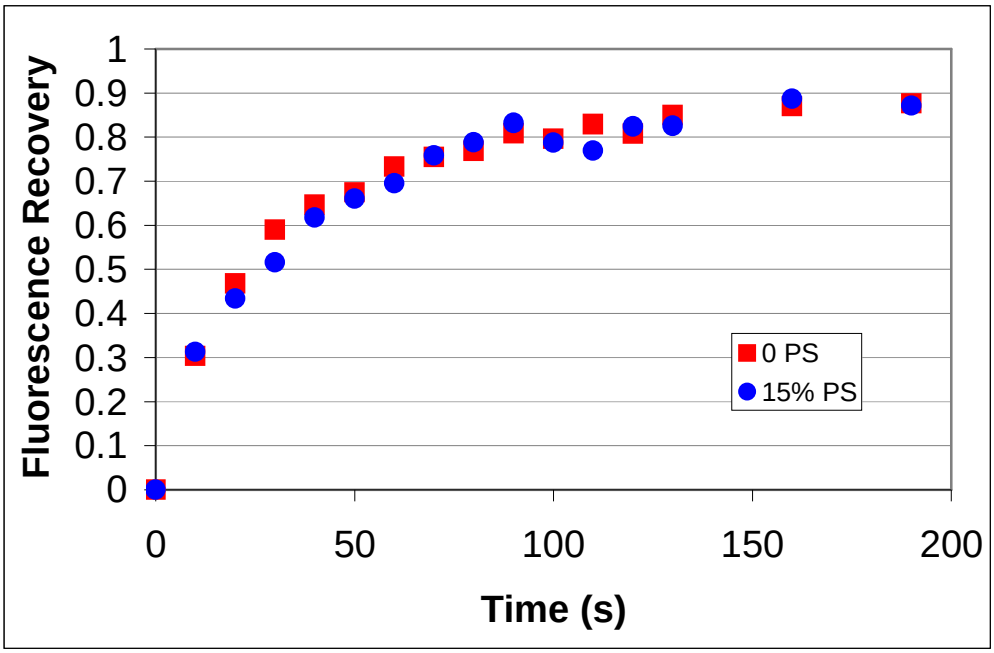

Figure S10. Typical fluorescence recovery after photobleaching (FRAP) curves obtained for an SLB containing 1 mol% TR-DHPE, 99 mol% POPC, and no PS (red) and 1 mol% TR-DHPE, 84 mol% POPC, and 15 mol% DOPS (blue) in a pH 7.4 citrate/Tris buffer (1 mM). The calculated diffusion constant was ~1.7 $\mu m^2/s$. The mobile fraction was generally observed to be greater than 0.9, although at the highest concentrations of PS (30 mol%) 0.8-0.85 mobile fractions were observed.

Supplementary Table S1: ICP-MS results of the nanopure water used in all the exp.

Nanopure water used in exp. (All in pM)	
Cu	<0.01
Mg	<0.01
Ni	2
Zn	60
Br	<0.1
P	<0.1
Cl	4000
K	6
Fe	100

The ICP-MS data of the nanopure water used in the experiments were collected on Perkin Elmer DRCII ICP-MS with both solution and laser ablation capabilities.

Supplementary Table S2: Lipids and Fluorophores Tested

Lipids Tested		Fluorophores Tested
Quenches TR-DHPE	Does not quench TR-DHPE	(All quenched by DOPS)
DOPS	GM1	TR-DHPE (ortho- and para-isomers, mixed or separate)
DLPS	DOPG	16:12 Tail-Labeled NBD PC
DPPS	DPPG	16:12 Tail-Labeled NBD PS
	POPG	18:1 Head-Labeled NBD PS
	Cardiolipin	Rhodamine-DHPE
	DOPA	Fluorescein-DHPE
	DSPA	Bodipy-DHPE

Quenching was determined for the lipids in column 1 (PS lipids) and column 2 (non-PS lipids) by the observed fluorescence difference between the lipid present and absent at pH 3.6 and 8.0. The PS species were tested at 15 mol% and all quenched TR-DHPE present at 1 mol%. For the non-quenching lipids, the concentrations tested were either 5 mol% (GM1 and cardiolipin) or 15 mol% (the other lipids). Again, the dye employed was TR-DHPE present at 1 mol%.

The fluorophores were tested at 1 mol% (TR-DHPE, Rhodamine-DHPE, Fluorescein-DHPE, 16:12 tail-labeled NBD PC, 16:12 tail-labeled NBD PS and 18:1 head-labeled NBD PS) or 2 mol% (Bodipy-DHPE), with 15 mol% DOPS-containing bilayers compared to bilayers containing no DOPS. In both cases, the balance of the SLB

consisted of POPC. Moreover, 10 mM sodium citrate/Tris buffers were used with 800 pM $CuSO_4$ in all cases.

A List of Chemical name

Abbreviation	Chemical name
DOPS	1,2-dioleoyl-*sn*-glycero-3-phospho-L-serine
DLPS	1,2-dilauroyl-*sn*-glycero-3-phospho-L-serine
DPPS	1,2-dipalmitoyl-*sn*-glycero-3-phospho-L-serine
GM1	mixed gangliosides, purified, bovine
Cardiolipin	1,1',2,2'-tetramyristoyl cardiolipin
DOPG	1,2-dioleoyl-*sn*-glycero-3-phospho-(1'-*rac*-glycerol)
DPPG	1,2-dipalmitoyl-*sn*-glycero-3-phospho-(1'-*rac*-glycerol)
POPG	1-palmitoyl-2-oleoyl-*sn*-glycero-3-phospho-(1'-*rac*-glycerol)
DOPA	1,2-dioleoyl-*sn*-glycero-3-phosphate
DSPA	1,2-distearoyl-*sn*-glycero-3-phosphate
TR-DHPE	Texas Red 1,2-dihexadecanoyl-*sn*-glycero-3-phosphoethanolamine
16:12 tail-labeled NBD PC	(1-palmitoyl-2-{12-[(7-nitro-2-1,3-benzoxadiazol-4-yl)amino]dodecanoyl}-*sn*-glycero-3-phosphocholine
16:12 tail-labeled NBD PS	1-palmitoyl-2-{12-[(7-nitro-2-1,3-benzoxadiazol-4-yl)amino]dodecanoyl}-*sn*-glycero-3-phosphoserine
18:1 head-labeled NBD PS	1,2-dioleoyl-*sn*-glycero-3-phospho-L-serine-N-(7-nitro-2-1,3-benzoxadiazol-4-yl)

Rhodamine-DHPE	Lissamine Rhodamine B 1,2-dihexadecanoyl-*sn*-glycero-3-phosphoethanolamine
Fluorescein-DHPE	N-(Fluorescein-5-thiocarbamoyl)-1,2-dihexadecanoyl-*sn*-glycero-3-phosphoethanolamine
Bodipy-DHPE	(N-(4,4-difluoro-5,7-dimethyl-4-bora-3a,4a-diaza-s-indacene-3-propionyl)-1,2-dihexadecanoyl-*sn*-glycero-3-phosphoethanolamine

Image Processing

Line scans of images were exported to Excel, where peak heights were determined by subtracting the average of the PDMS-glass junction fluorescence intensity on either side of a channel from the average intensity inside of the channel itself. The variation reported in the paper, particularly in Figure 3, is the variation observed between multiple measurements. The number of measurements varied, but typically was between three and seven.

$CuSO_4$ Extrusion with Vesicles

As noted in the experimental section, $CuSO_4$ was generally added to the buffer for measurements of fluorescence quenching in 100 nm vesicles with 15 mol% DOPS (Figure 5). As a control, experiments were also performed by introducing $CuSO_4$ after vesicle extrusion. This should only quench fluorophores on the outer leaflet. Indeed, quenching was diminished in such controls, but by usually less than a factor of two. This may be due to a preferential partitioning by Texas Red DHPE to the outer leaflet of the vesicles, since the head group larger is larger than the surrounding POPC lipids. Also, the surface area of the outer leaflet is somewhat greater than the inner leaflet in 100 nm vesicles. Finally, some leakage of the vesicles could also cause the quenching difference to be somewhat less than a factor of two.

References

(1) Crane, J. M.; Tamm, L. K *Biophys. J.* **2004**, *86*, 2965.

(2) Lakowicz, J. R. *Principles of Fluorescence Spectroscopy*; 3rd Edition ed.; Springer Science+Business Media: New York, 2006.

(3) Shi, J. J.; Yang, T. L.; Kataoka, S.; Zhang, Y. J.; Diaz, A. J.; Cremer, P. S. *J. Am. Chem. Soc.* **2007**, *129*, 5954.

(4) Lencer, W. I.; Chu, S. H. W.; Walker, W. A. *Infect. Immun.* **1987**, *55*, 3126.

(5) Job, P. *Ann. Chim.* **1928**, *9*, 113.

(6) Jastrzab, R.; Lomozik, L. *J. Coord. Chem.* **2009**, *62*, 710.

(7) Várnagy, K.; Garribba, E.; Sanna, D.; Sóvágó, I.; Micera, G. *Polyhedron* **2005**, *24*, 799.